Induction of T-Cell Infiltration and Programmed Death Ligand 2 Expression by Adeno-Associated Virus in Rhesus Macaque Skeletal Muscle and Modulation by Prednisone

Megan L. Cramer,[1] Guohong Shao,[2,3] Louise R. Rodino-Klapac,[2,3] Louis G. Chicoine,[2,3] and Paul T. Martin[2,3,*]

[1]Molecular, Cellular, and Developmental Biology Graduate Program, The Ohio State University, Columbus, Ohio; [2]Center for Gene Therapy, The Research Institute at Nationwide Children's Hospital, Columbus, Ohio; [3]Department of Pediatrics, The Ohio State University College of Medicine, Columbus, Ohio.

Use of adeno-associated virus (AAV) to transduce genes into skeletal muscles can be associated with T-cell responses to viral capsid and/or to transgenic protein. Intramuscular mononuclear cell infiltrates primarily consisting of CD8+ T cells and also containing FOXP3+ regulatory T cells were present in rhesus macaque skeletal muscle treated with rAAVrh74.MCK.*GALGT2* by vascular delivery. Administration of oral prednisone prior to AAV gene delivery and throughout the study reduced such infiltrates by 60% at 24 weeks post AAV delivery compared with AAV-treated animals not receiving prednisone, regardless of the presence of pre-existing AAV serum antibodies at the time of treatment. The majority of CD8+ T cells in AAV-treated muscles expressed activated caspase 3 and programmed cell death protein 1 (PD1), suggesting ongoing programmed cell death. AAV-transduced skeletal muscles also had elevated expression of programmed death ligand 2 (PDL2) on skeletal myofibers, and this increase in expression extended to muscles where transgene was not overexpressed. These data demonstrate that prednisone can reduce the extent of intramuscular T-cell infiltrates in AAV-treated muscles, which may aid in achieving long-term transgene expression, as may the induction of PDL2 expression on skeletal myofibers to promote PD1-mediated programmed T-cell death.

Keywords: gene therapy, AAV, PD1, muscular dystrophy, neuromuscular junction, lymphocyte

INTRODUCTION

ADENO-ASSOCIATED VIRUS (AAV) has increasingly become the viral vector of choice for gene therapy clinical trials.[1] The advantages of using AAV include the episomal nature of the introduced gene, which allows for sustained transgene expression in postmitotic cells, the relative ease with which certain AAV serotypes can cross the vascular barrier to transduce multiple tissues, and the benign, nonpathogenic nature of AAV as an infectious agent. There are, however, significant obstacles posed by the host immune system to the successful use of AAV.[2]

One obstacle to AAV treatment is the induction of CD8+ cytotoxic T cells.[3] T-cell clones specific to peptides within the AAV capsid protein or to peptides from the protein produced by the delivered transgene can weaken the expression of the therapeutic transgene over time.[1] High *et al*. demonstrated that hemophilia B patients treated with factor IX gene therapy developed positive T-cell responses in peripheral blood mononuclear cells (PBMCs) to the AAV8 capsid protein, and this sometimes coincided with elevated serum liver enzymes and lowered factor IX expression.[4] The presence of capsid-responsive T cells, however, does not necessarily eliminate AAV-mediated transgene expression. Brantly *et al*. showed that patients with α1 anti-trypsin (AAT) deficiency treated by intramuscular injection of AAV1-AAT were able to maintain transgene expression a year after injection, despite the presence of T-cell responses to rAAV1 capsid peptides.[5] Thus, some tolerance or exhaustion may occur in AAV-targeted

*Correspondence: Dr. Paul Martin, Department of Pediatrics, The Ohio State University College of Medicine, 700 Children's Drive, Columbus, OH 43205. E-mail: paul.martin@nationwidechildrens.org

DOI: 10.1089/hum.2016.113

T-cell populations. Additional studies in humans and in animal models of disease have implicated both CD8+ and regulatory T cells (Treg) as effectors of AAV-mediated transgene expression.[6–11] Such T-cell responses can be reduced by treatment with immunosuppressants such as prednisone, mycophenolate mofetil, tacrolimus, and daclizumab.[12–14]

Another obstacle to AAV-mediated gene expression is the blockage of AAV entry into cells by pre-existing serum antibodies to the viral capsid protein. Humans show differential rates of infection to various AAV serotypes. For example, human antibody titers are more commonly found to rAAV2[15] than to rAAV9.[15,16] Such differences can vary by geographic location and by age,[17] but anti-AAV capsid antibodies exist in a significant fraction of humans due to previous exposure to AAV. Serum antibodies to AAV are induced in all patients and animal models after AAV administration and can typically block subsequent AAV transduction once present.[16,18] Serum antibodies to the introduced transgenic protein may also occur and are more common in animals undergoing gene replacement where the endogenous gene is deleted.[6,9] A variety of methods exist to reduce B cells or B-cell antibody production (*e.g.*, rituximab[10,19,20] and rapamycin[6,21]) or serum antibody levels (*e.g.*, plasmapheresis[22,23]), all of which can alleviate serum antibody blockage of AAV-mediated transgene expression.

In the development of rAAVrh74.MCK.*GALGT2* gene therapy for the treatment of Duchenne muscular dystrophy (DMD), both cellular and humoral immune barriers to transgene expression in the skeletal muscles of nonhuman primates have been encountered.[24] rAAVrh74.MCK.*GALGT2* is a gene therapy vector that utilizes the muscle creatine kinase (MCK) promoter to confine *GALGT2* (now *B4GALNT2*) gene expression to skeletal and cardiac muscle and uses the rhesus 74 serotype of AAV, an AAV8-like serotype that allows for capsid delivery to tissues via the blood.[25] *GALGT2* encodes the β1-4 N-acetylgalactosaminyltransferase needed to make the cytotoxic T-cell (CT) glycan (Neu5Acα2–3[GalNAcβ1–4]Galβ1–4GlcNAcβ-), also called the Sda or Cad blood group antigen, on certain glycoproteins and glycolipids.[26] Despite its original identification in CD8+ T cells, *GALGT2* is most highly expressed in the human colon.[26,27] In adult skeletal muscle, *GALGT2* expression is confined to the neuromuscular junction (NMJ) and the myotendinous junction (MTJ).[28,29] When overexpressed, however, *GALGT2* induces CT glycan overexpression along the entirety of the muscle membrane and also induces the overexpression of a group of glycoproteins normally confined to the NMJ and MTJ, including agrin, laminin α5, utrophin, and plectin 1.[30–32] Overexpression of these genes in skeletal muscle can ameliorate muscular dystrophy in several different genetic forms of the disease,[24,33,34] while deletion can increase disease severity.[35–38] *GALGT2* overexpression has been shown to inhibit the development of muscular dystrophy in the *mdx* model for DMD, the dy^W model for congenital muscular dystrophy 1A, the $Sgca^{-/-}$ model for limb girdle muscular dystrophy 2D, and the *FKRP* P448L model for limb girdle muscular dystrophy 2I.[31,32,39–41]

While several genes, including *GALGT2*, have shown promise in small animal models of muscular dystrophy, attempts to move a therapeutic vector to nonhuman primates and subsequently to human clinical trials have had setbacks due to the induction of deleterious T-cell responses to the viral capsid proteins and to the delivered transgene product.[1,2] It was recently shown that vascular delivery of AAV to the gastrocnemius muscle of rhesus macaques could result in expansive *GALGT2* gene expression lasting for at least 6 months.[30] Gene expression, however, depended heavily on the absence of pre-existing rAAVrh74 serum antibodies, as animals with high titers (seropositive) had significantly lower *GALGT2* expression.[30] CD8+ T-cell infiltrates were occasionally present in treated muscles, and PBMC interferon gamma (IFN-γ) responses to viral capsid and transgene peptides were also present.[30] This study sought to explore the molecular underpinnings that might allow for continued transgene expression in the face of such T-cell-mediated immunity, including T-cell exhaustion.

A number of different viruses are able to induce immunologic exhaustion in their host.[42] Viruses often stimulate T-cell exhaustion by inducing expression of programmed cell death protein 1 (PD1) on the surface of T cells.[43] Lymphocytic choriomeningitis virus, hepatitis virus, and recombinant adeno-associated virus (rAAV) have all been shown to induce PD1 expression on CD8+ T cells after infection.[42–44] Immune function can be restored in exhausted T cells by suppressing PD1 signaling.[44] Loss of PD1 in the mouse also increases the incidence of autoimmunity, including lupus-like arthritis and glomerulonephritis. When crossed into other backgrounds, loss of PD1 can increase graft-versus-host disease,[22,45] again pointing to a central role for PD1 in controlling T-cell-mediated immunity. PD1 activation on T cells can be accomplished by binding to one of its two known PD1 ligands, programmed death ligand 1 (PDL1) or PDL2.[43] Both PD1 ligands are expressed in a variety of non-lymphoid tissues, and

PDL2 is more highly expressed than PDL1 in human and mouse skeletal muscle.[46] Here, the expression of PD1 and its two known ligands have been studied in rAAVrh74.MCK.*GALGT2*-treated macaque skeletal muscle. In addition, the impact of prednisone, an immune suppressant commonly used as a standard of care in DMD,[47] on the presence of intramuscular T-cell infiltrates has been investigated.

METHODS

Rhesus macaques

All procedures were performed with the approval of the Institutional Animal Care and Use Committee at the Research Institute at Nationwide Children's Hospital.

AAV production

rAAVrh74.MCK.*GALGT2* and rAAVrh74.MCK.μDystrophin were produced by the Viral Vector Core at Nationwide Children's Hospital using methods and primers, as previously described.[30] rAAV was produced by standard triple transfection method in HEK293 cells,[48] with purification of packaged vector by sucrose density centrifugation and anion exchange chromatography, as previously described.[49]

Isolated focal limb perfusion

Muscles were analyzed from experiments described in a previous study.[30] Briefly, 2×10^{12} vg/kg of rAAVrh74.MCK.*GALGT2* or 2×10^{12} vg/kg rAAVrh 74.MCK.μDystrophin was infused in 2.5 mL/kg of normal saline using a fluoroscopy-guided catheter to deliver AAV vector to the gastrocnemius muscle via the femoral artery through the sural branch of the popliteal artery. The catheter was inserted into the femoral artery via an incision site in the groin area. The gastrocnemius muscle was isolated by the presence of two standard phlebotomy tourniquets, one placed above the right knee just proximal to the tip of the catheter and one placed just below the gastrocnemius muscle. Prior to vector administration, a flush of saline (2.5 mL/kg) was delivered over 1 min, after which vector was infused over 1 min in an identical volume and allowed to dwell in the limb for 10 min. This was followed by an additional flush of 2.5 mL/kg of normal saline delivered over 1 min, after which the tourniquets were released and the catheter removed. Residual bleeding was stopped by applied pressure, and the incision was closed by suturing. All treated macaques were sacrificed at either 12 or 24 weeks post injection. Gastrocnemius muscles from each animal were removed and divided into 13–16 segments (0.75–1.0$\times$0.5 cm blocks). Blocks were embedded in 7% gum tragacanth and snap-frozen in liquid nitrogen–cooled isopentane.

Anti-AAV serum antibody titers

Macaques were divided into seronegative groups and seropositive groups, depending on the presence of a twofold elevation in rAAV antibody titer at a dilution of 1:50 compared to wells containing no AAV using an enzyme-linked immunosorbent assay (ELISA). Macaques were considered AAV seronegative if they had no measurable antibody titer to rAAVrh74 using a 1:50 serum dilution. Absolute serum antibody titer signals at a 1:800 dilution were also compared for seropositive and seronegative groups. Serostatus cutoff measures were based on previous studies that assessed the relationship between muscle transgene expression and total serum antibody ELISA values.[23,30]

Prednisone treatment

Two weeks prior to rAAVrh74.MCK.*GALGT2* injection, one cohort of macaques was given daily doses of prednisone (0.75 mg/kg/day), and this treatment regimen was continued for the full 24 weeks after AAV delivery.

Lectin staining to measure GALGT2 activity in transduced muscles

Frozen cross-sections of skeletal muscle (10 μm thick) were cut on a cryostat, blocked in 10% donkey serum, and probed with biotinylated *Wisteria floribunda* agglutinin (WFA; Vector Laboratories, Burlingame, CA). Sections were later incubated with streptavidin-conjugated secondary antibody (Jackson ImmunoResearch Laboratories, West Grove, PA) and mounted with ProLong Gold Antifade Mountant with DAPI (Thermo Fisher Scientific, Carlsbad, CA). A Zeiss Axioskop2 Plus epifluorescence microscope was used to visualize staining, and a Zeiss AxioCam MRC5 camera (Carl Zeiss Microscopy, Thornwood, NY) was used to capture four representative 10$\times$images (each 977,500 μm^2 in area) per muscle block, for which the exposure was time-matched between all cohorts. The percentage of fibers that stained with WFA was calculated relative to the total myofibers in each image and averaged for each cohort. Both the medial and lateral heads of each gastrocnemius muscle were analyzed, with 13–16 blocks analyzed per muscle head and two to three animals analyzed per condition. There were 90–120 images analyzed per macaque, with each image having about 350 myofibers. Investigators were blinded to conditions, and a 16% inter-investigator error was calculated between those who counted the same images. Significant differences between the average WFA expression for each cohort were

determined using an ordinary one-way analysis of variance (ANOVA) and Sidak's multiple comparisons test.

Quantitative polymerase chain reaction to detect viral genomes

TaqMan quantitative polymerase chain reaction (qPCR) was used to quantify AAV vector genome copies in treated gastrocnemius muscles and saline-treated control muscles. Genomic DNA was extracted as previously described[30] from seven different muscle blocks spaced throughout the rostral–caudal axis of each head of the gastrocnemius muscle. DNA purity and quantity was measured using an ND-1000 spectrophotometer (NanoDrop; Thermo Fisher Scientific). A vector-specific primer/probe set (forward: 5′-CCTCAGTG GATGTTGCCTTTA, probe: 5′-AAAGCTGCG/ZEN/ GAATTGTACCCGC/3IABkFQ, and reverse: 5′-AT CTTGAGGAGCCACAGAAATC) was used to amplify a portion of the vector DNA encompassing the 3′ end of the MCK promoter and the 5′ end of the human *GALGT2* cDNA. No amplification of the endogenous macaque (*Macaca mulatta*) *GALGT2* was observed in control samples using this vector-specific primer/probe set. The plasmid used to make rAAVrh74.MCK.*GALGT2* was linearized with ClaI, repurified, and utilized to generate a standard curve from 50 to 5 million copies in log increments. The correlation coefficient of the standard curve always equaled or exceeded 0.99. Copy number was reported as vector genomes per microgram of genomic DNA assayed. Each sample was measured in duplicate, with an average intra-sample error of 8%. Values for each cohort were averaged, and differences between the cohorts were analyzed using an ordinary one-way ANOVA and Sidak's multiple comparisons test.

Semi-quantitative reverse transcription PCR

Relative transcription levels were assessed by quantitative reverse transcription PCR (qRT-PCR) using the $\Delta\Delta$CT method,[50] with 18S ribosomal RNA as an internal reference. Total RNA was isolated from gastrocnemius muscle blocks using Trizol reagent (Invitrogen Life Technologies, Grand Island, NY) and purified on a silica gel–based membrane (Direct-zol RNA miniPrep; Zymo Research, Irvine, CA). RNA purity and content was measured using an ND-1000 spectrophotometer (NanoDrop; Thermo Fisher Scientific). RNA was reverse transcribed with a high capacity cDNA archive kit (Applied Biosystems, Thermo Fisher Scientific) per the manufacturer's guidelines. Using a TaqMan ABI 7500 sequence detection system (Applied Biosystems, Thermo Fisher Scientific) with 18S as an internal reference, samples underwent RT-PCR in duplicate. Primer/probe sets were designed using PrimerQuest DNA software and synthesized by Integrated DNA Technologies (Coralville, IA). A primer/probe set for 18S was purchased from Applied Biosystems (Thermo Fisher Scientific) and primer/probe sets were designed only to recognize *Homo sapiens GALGT2* (CTACGATG GAATCTGGCTGTT (forward), 56-FAM/AGCCAAC AA/Zen/AGAGCAGGGAGGTTA/3IABkFQ (probe), GCCATAGGCATCCTGAAAGT (reverse)) or *Macaca mulatta GALGT2* (TGAGGAGACAGGCTGAATTTG (forward), 56 FAM/ACTTTCAGA/Zen/GGAGAGAA GGGCTGC/3IABkFQ (probe), TCCATTGATGACGA GCTTCC (reverse)). Human *GALGT2* levels were then compared to rhesus macaque *GALGT2* levels in each sample. Relative mRNA levels were averaged for each cohort and analyzed using an ordinary one-way ANOVA and Sidak's multiple comparisons test.

Scoring of intramuscular immune cell infiltrates

Snap-frozen blocks of skeletal muscle were cut on a cryostat to create cross-sections (10 μm thick), which were then stained with hematoxylin and eosin (H&E). For H&E staining, sections were fixed in 10% neutral buffered formalin, stained in Gill's 3 Hematoxylin (Fisher Scientific, Pittsburgh, PA), immersed in bluing reagent, stained with eosin (Fisher Scientific), and dehydrated in increasing concentrations of ethanol and, lastly, xylene. A Zeiss Axioskop40 microscope (Carl Zeiss Microscopy) was used to capture five representative $10\times$ images (each 977,500 μm^2 in area) from one H&E-stained section for each of the 13–16 blocks taken from each head of the gastrocnemius muscle. Each image was given a score reflecting the percentage of infiltration by mononuclear cells, termed the infiltration index. These scores were given as follows: "0" for infiltration in 0% of total cellular area in the image, "1" for $0\% < x \leq 5\%$, "2" for $5\% < x \leq 15\%$, and "3" for $15\% < x \leq 25\%$. No infiltration above 25% of the total cellular area was observed. Approximately 150 images per animal were analyzed in this manner. Infiltration index scores for each treatment group were then averaged and analyzed for differences using an ordinary one-way ANOVA and Sidak's multiple comparisons test.

IFN-γ Enzyme-Linked ImmunoSpot assays

Enzyme-Linked ImmunoSpot (ELISpot) assays were performed on fresh PBMCs, which were added at 2×10^5 cells/well to duplicate wells of a 96-well plate. Three peptide pools were used for the rAAVrh74 capsid protein sequence. Each

contained 34–36 peptides of 18 amino acids in length, with each peptide overlapping in sequence with the previous peptide by 11 residues. Two peptide pools of a similar nature were used to assay the human GALGT2 protein sequence. Concanavalin A (ConA) was used as a positive control and vehicle (0.25% dimethyl sulfoxide [DMSO]) was used as a negative control. Peptides were added at 1 mg/mL to Aim-V lymphocyte media (Invitrogen Life Technologies) supplemented with 2% human AB serum (Gemini-BioScience, Liverpool, United Kingdom). Monkey IFN-γ ELISpot kits were purchased from U-CyTech (Utrecht, The Netherlands). After addition of PBMCs and peptides, the plates were incubated at 37°C for 48 hours and developed according to the manufacturer's instructions. Spot formation was counted using a Cellular Technologies Systems analyzer (Cleveland, OH).

Immunostaining

Sections of skeletal muscle (10 μm thick) were blocked in 10% donkey serum and probed with biotinylated *Wisteria floribunda* agglutinin (WFA; Vector Laboratories), monoclonal antibody to cleaved caspase 3 (Asp 175; 5A1E; Cell Signaling, Danvers, MA), monoclonal antibody to the FLAG epitope tag (M2; Sigma–Aldrich, St. Louis, MO), monoclonal antibody to CD4 (L200; BD Biosciences, San Jose, CA), monoclonal antibody to CD8 (YTC182.20; AbD Serotec, Raleigh, NC), monoclonal antibody to CD11b (EP1345Y; Abcam, Cambridge, MA), monoclonal antibody to FOXP3 (236A/E7) (Abcam), PD1/CD279 antibody (Thermo Fisher Scientific), PDL1 antibody (EMD Millipore, Billerica, MA), PDL2 antibody (EMD Millipore), or monoclonal antibody to reticular fibroblasts and reticular fibers (ERTR7; Abcam). Sections were then incubated in fluorophore-conjugated secondary antibody, fluorophore-conjugated streptavidin (Jackson ImmunoResearch Laboratories) or fluorophore-conjugated α-bungarotoxin (Thermo Fisher Scientific). Stained slides were mounted with ProLong Gold Antifade Mountant with DAPI (Thermo Fisher Scientific). A Zeiss Axioskop2 Plus epifluorescence microscope was used to visualize staining and a Zeiss AxioCam MRC5 camera (Carl Zeiss Microscopy) was used to capture representative images. All images comparing individual stains between different experimental conditions or animals were time-matched using identical exposure settings.

Western blot analysis

Frozen skeletal muscle blocks were cut on a cryostat (50 μm/section) to obtain roughly 50 mg of muscle protein per sample. Muscle was digested in Tris-buffered saline (TBS; 25 mM of Tris, 150 mM of NaCl, pH 7.5) containing 1% NP-40, 0.5 mM of EDTA, and 1:50 cOmplete protease inhibitors (Roche, Indianapolis, IN) overnight. Extracts were homogenized with three to five pulses of 10 s each (Power Gen 125; Fisher Scientific). Samples were centrifuged at 21,000 *g* for 30 min at 4°C to remove unsolubilized material. The supernatant was collected, and the resulting protein concentration was determined by BCA assay (Thermo Fisher Scientific). Protein (80 μg) from each sample was boiled at 100°C for 10 min in NuPAGE LDS sample buffer (Thermo Fisher Scientific), separated on a Bolt 4–12% Bis-Tris Plus gel (Thermo Fisher Scientific), and transferred to a nitrocellulose membrane. The membrane was blocked in 5% nonfat dry milk in TBS containing 0.05% Tween 20 and then probed with PD1/CD279 antibody (Thermo Fisher Scientific), PDL1 antibody (EMD Millipore), PDL2 antibody (EMD Millipore), or GAPDH antibody (Sigma–Aldrich). Blots were then probed with horseradish peroxidase–coupled secondary antibody (Jackson ImmunoResearch Laboratories) and developed using the enhanced chemiluminescence (ECL) method (Lumigen, Southfield, MI). ImageJ 1.46r software (National Institutes of Health, Bethesda, MD) was used to measure relative band density in the 24-week rAAV74.MCK.*GALGT2*-treated macaque muscle samples (with or without prednisone), contralateral control limb muscle samples, and sham-treated control muscle samples. PD1, PDL1, and PDL2 protein expression were normalized to GAPDH expression in each instance ($n = 6$ per cohort). Densitometry measures for each cohort were averaged, and variation between cohorts was analyzed using an ordinary one-way ANOVA and Sidak's multiple comparisons test.

RESULTS

Vascular delivery of rAAVrh74.MCK.*GALGT2* to skeletal muscle

Skeletal muscles from a previous gene therapy study were also used in the current study.[30] In that study, a 2×10^{12} vg/kg dose of either the human *GALGT2* gene or the micro-Dystrophin (μDys) gene was delivered to the gastrocnemius muscle in a single limb using an isolated limb perfusion method with intra-arterial delivery in rhesus macaques. At endpoints of 12 and 24 weeks post injection, both the treated and the contralateral gastrocnemius muscles were removed and snap-frozen for further analysis, along with skeletal muscle from a phosphate-buffered saline (PBS)-injected macaque (sham control). Muscles were

dissected into 13–16 blocks of tissue taken equally from the proximal, central, and distal regions of the lateral and the medial heads of the gastrocnemius. After snap-freezing, rAAVrh74.MCK.*GALGT2*-treated blocks were cut into cross-sections and immunostained to analyze the extent of *GALGT2* transduction.

For the current study, macaques treated with human *GALGT2* were divided into five experimental groups depending on the length of treatment, AAV serostatus at the time of treatment, and the presence or absence of prednisone as an additional treatment. Macaques were considered AAV seronegative if they had no measurable antibody titer to rAAVrh74 using a 1:50 serum dilution by ELISA. It is important to point out that the serum rAAV antibody titer was a measure of total rAAVrh74 antibodies and not a measure of neutralizing AAV antibodies. The control group (group 1) was injected with normal saline. Of the four rAAVrh74.MCK.*GALGT2*-treated experimental groups, group 2 was analyzed at 12 weeks post treatment, and groups 3–5 were analyzed at 24 weeks post treatment. Group 3 received no prednisone and had no measurable serum rAAV antibody titer at the time of treatment (sero–). Group 4 had positive serum rAAV antibody titers at the time of treatment (sero+) and received prednisone, while group 5 was rAAV antibody seropositive (sero+) but did not receive prednisone. At the time of treatment, the seropositive groups had average serum rAAVrh74 antibody ELISA signals of 0.336 (group 4) or 0.288 (group 5) using a 1:800 serum dilution, while the seronegative groups had average serum rAAVrh74 antibody ELISA signals of 0.057 (group 2) or 0.028 (group 3).

In each treated group, the gastrocnemius muscles from the treated limb and from the contralateral (untreated) limb were analyzed for GALGT2 activity using WFA staining (Fig. 1A). WFA recognizes the terminal β1-4GalNAc linkage that is unique to the CT glycan structure and therefore can be used to recognize the product of GALGT2 enzyme activity.[28,30] *GALGT2* gene overexpression is easily scored in this manner, as CT glycan expression, like GALGT2 protein, is normally confined to the NMJ and MTJ in adult skeletal muscle (and in some intramuscular capillaries).[28,29] By contrast, when *GALGT2* is overexpressed in skeletal muscle, the CT glycan is present along the entirety of each transduced myofiber membrane.[30] Contralateral (control) muscles showed almost no (<1% of total myofibers) CT glycan staining along myofibers, while rAAVrh74.MCK.*GALGT2*-treated muscles had *GALGT2* overexpression in 56 ± 9% of myofibers at 12 weeks (group 2) and 34 ± 19% (group 3), 57 ± 7% (group 4), and 12 ± 2% (group 5) at 24 weeks (data are mean ± standard deviation [*SD*]; Fig. 1B). The presence of pre-existing antibodies to AAV significantly reduced CT glycan overexpression in group 5 relative to group 2 and to group 4 ($p < 0.05$). Group 4, which also had pre-existing Abs but received prednisone treatment, did not have CT glycan overexpression that was significantly different from the two seronegative cohorts (groups 2 and 3). WFA staining in myofibers was much more variable in the 24-week-treated group without prednisone (group 3) due to the presence in this cohort of one macaque with a Mamu-A0201 class I allele.[30] This allowed for T-cell responses to a GALGT2 peptide with human-specific amino-acid changes relative to the macaque sequence, resulting in transient breakage of T-cell tolerance to the transgenic protein at 20 weeks post treatment.[30] While not proven, this could have contributed to the significantly lowered CT glycan expression in this particular animal, which increased the variability of WFA staining in the group 3 cohort.

Next, qPCR analysis was performed to measure the number of viral genomes present in each treated skeletal muscle (Fig. 1C). Seropositive AAV-treated macaques, with or without prednisone (groups 4 and 5), showed a reduction in viral genomes per microgram of genomic DNA relative to seronegative macaques at 12 or 24 weeks post treatment, though this reduction was only significant compared with the 12-week-treated group 2 cohort ($p < 0.05$). Despite the reduction in viral genomes, group 4 showed increased transgene expression by qRT-PCR relative to the seronegative cohort treated similarly for 24 weeks (group 3; Fig. 1D). Additionally, group 2 had significantly higher *hGALGT2* mRNA expression relative to groups 3 and 5 ($p < 0.05$ and $p < 0.01$, respectively; Fig. 1D). The increase in group 4 h*GALGT2* mRNA expression, which may result from prednisone activation of the MCK promoter or stabilization of the *GALGT2* mRNA, could in part account for the increased percentage of myofibers overexpressing the CT glycan in group 4 relative to group 5 (Fig. 1B). Additional effects of prednisone, for example, on GALGT2 protein expression, GALGT2 enzyme activity, or GALGT2 substrate expression or secretion may also be involved.

Prednisone suppresses T-cell infiltrates in AAV-transduced muscle

The presence of T-cell infiltrates in rAAVrh74.MCK.*GALGT2*-treated muscle sections was observed, as has been previously reported.[30] To

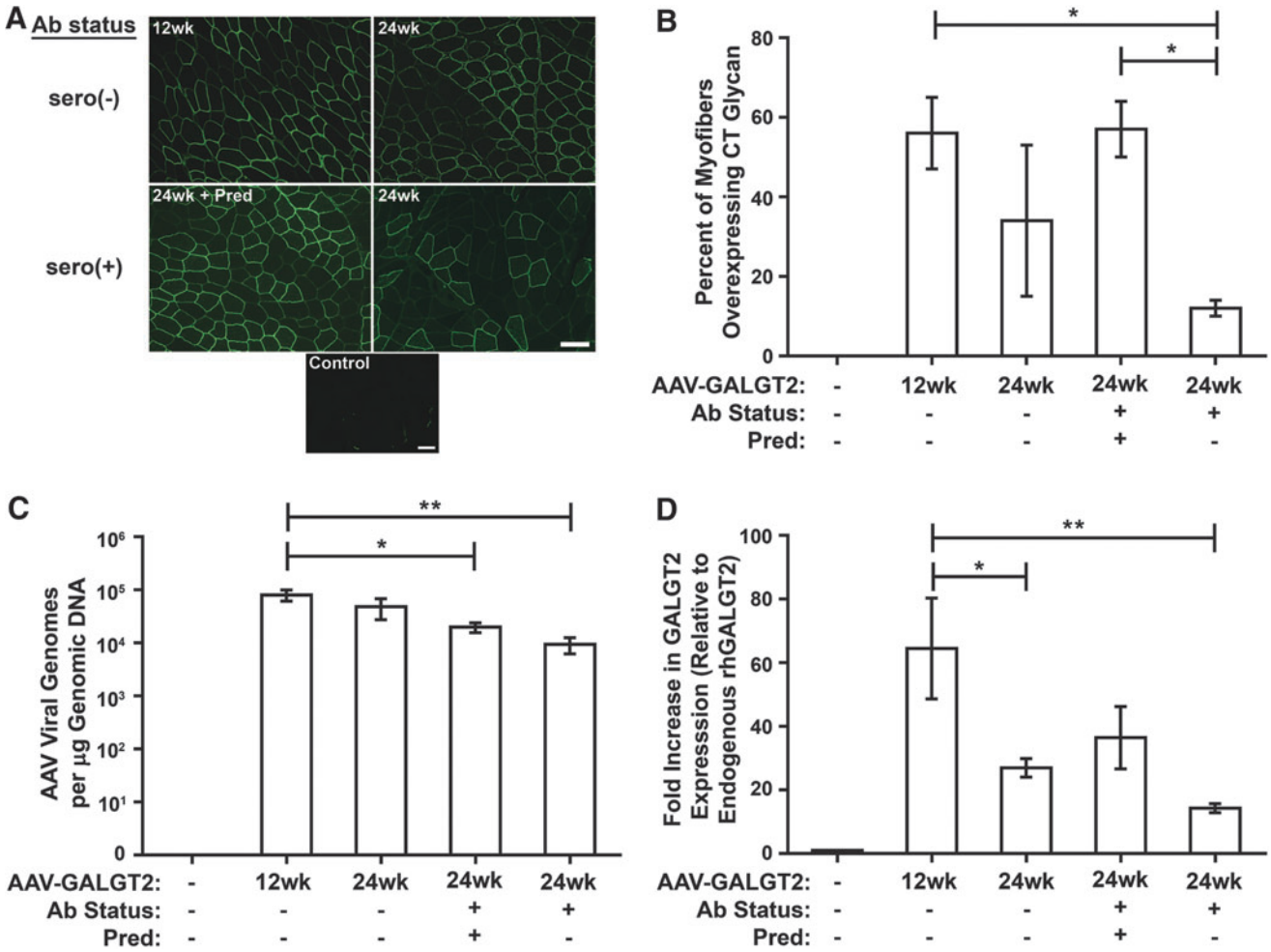

Figure 1. GALGT2 expression and adeno-associated viral (AAV) vector biodistribution after vascular delivery of rAAVrh74.MCK.*GALGT2*. (**A**) *GALGT2* overexpression is shown by *Wisteria floribunda* agglutinin (WFA) staining in rAAVrh74.MCK.*GALGT2*-treated gastrocnemius muscle in seronegative (–) or seropositive (+) macaques, of which one cohort was additionally treated with prednisone (Pred). Control represents time-matched WFA staining of an untreated muscle. Scale bar: 50 μm. (**B**) The percentage of myofibers overexpressing CT glycan was quantified for all muscle segments taken throughout both heads of the gastrocnemius muscle. Data are mean ± standard deviation (*SD*) for $n=2$ (group 5) and $n=3$ (groups 1–4) macaques per group. (**C**) AAV vector genomes were measured by quantitative polymerase chain reaction (qPCR) and normalized to total genomic DNA. Data are mean ± standard error of the mean (SEM) for seven muscle samples analyzed for two to three macaques per group. (**D**) Relative change in transgenic human *GALGT2* mRNA expression, compared to endogenous rhesus macaque *GALGT2* mRNA expression, was determined using quantitative reverse transcription PCR (qRT-PCR) with 18S ribosomal RNA as an internal reference. Data are mean ± SEM for seven muscles analyzed for two to three macaques per group. *$p<0.05$, **$p<0.01$ using one-way analysis of variance (ANOVA) in (**B**–**D**).

quantify the abundance of such cellular infiltrates, an infiltration index was created. In this index, a score reflecting the percentage of infiltration was given to each H&E-stained muscle section. "0" represented no evident mononuclear infiltrates, "1" represented infiltration in 0–5% of the muscle section, "2" represented infiltration in 5–15%, and "3" represented infiltration in 15–25%. No sections showed infiltrates in >25% of the total muscle section area. Representative examples of muscle sections stained from all AAV-treated cohorts are shown in Fig. 2A, while examples for each infiltration index score between "0" and "3" are shown in Fig. 2B. Mononuclear cell infiltrates were significantly more abundant in all AAV-treated cohorts that did not receive prednisone than in the one cohort that did ($p<0.001$; Fig. 2C). At 24 weeks post AAV treatment, administration of prednisone significantly reduced the presence of mononuclear T-cell infiltrates, showing an overall reduction of 60% compared with 24-week-treated cohorts either with or without pre-existing serum rAAVrh74 antibodies.

In addition to characterizing the effect of prednisone on the extent of intramuscular T-cell infiltrates, anti-rAAVrh74 antibodies in serum (Fig. 2D) and IFN-γ positive T cells in PBMCs (Fig. 2E and F) were also measured. While anti-rAAVrh74 capsid

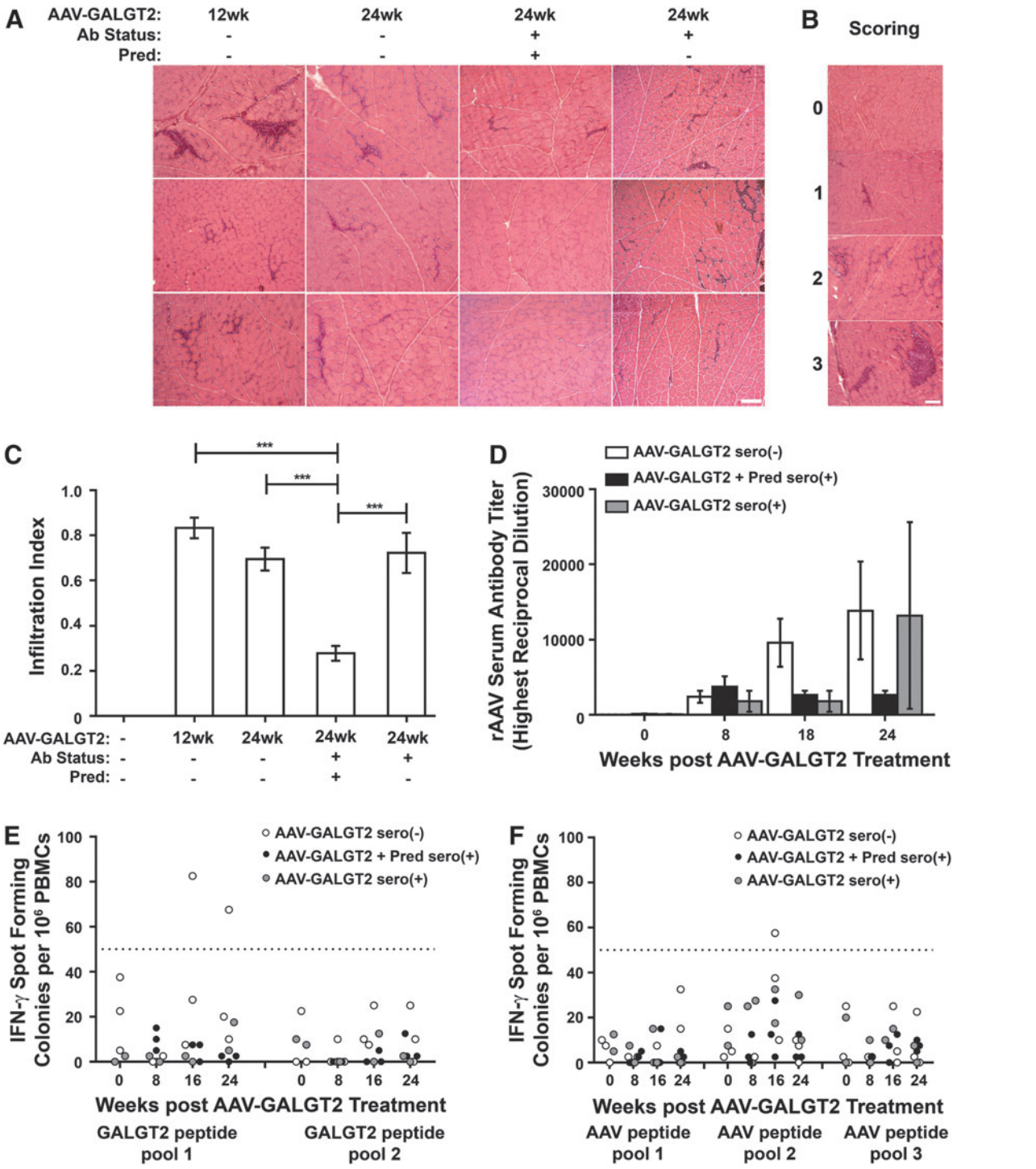

Figure 2. Prednisone reduces intramuscular T-cell infiltrates. (**A**) Hematoxylin and eosin staining of gastrocnemius muscles treated with rAAVrh74.MCK.*GALGT2* in the presence or absence of prednisone (Pred) and with or without pre-existing serum rAAV antibodies (Ab status + or –, respectively) at 12 and 24 weeks post injection. Scale bar: 100 μm. (**B**) Representative images reflecting infiltration index: "0" for 0% of imaged cellular area, "1" for $0\% < x \leq 5\%$, "2" for $5\% < x \leq 15\%$, and "3" for $15\% < x \leq 25\%$. Scale bar: 100 μm. (**C**) Average infiltration index for each rAAVrh74.MCK.*GALGT2*-treated cohort. Contralateral muscles from injected macaques were used as controls. Data are mean ± SEM with 150 images for $n=2$ (group 5) and $n=3$ (groups 1–4) macaques per group. ***$p<0.001$ using one-way ANOVA. (**D**) Anti-rh74 serum antibody levels in seronegative (–) and seropositive (+) 24-week rAAVrh74.MCK.*GALGT2*-treated macaques, with or without prednisone (Pred; $n=2$–3 per group). (**E**–**F**) Enzyme-Linked ImmunoSpot (ELISpot) peripheral blood interferon gamma (IFNγ) responses to GALGT2 peptides (**E**) or rAAVrh74 capsid peptides (**F**) in 24-week rAAVrh74.MCK.*GALGT2*-treated macaques. Each point represents one sample, with two to three macaques per group. IFN-γ responses were not determined at week 0 for the prednisone-treated cohort. Fifty spot forming colonies/10^6 peripheral blood mononuclear cells (PBMCs; line) is considered a positive response.

antibody levels were low prior to AAV treatment, levels rose following treatment and continued to rise at 18 and 24 weeks. At these later time points, the prednisone-treated cohort showed reduced serum antibody levels compared with animals not receiving prednisone, regardless of pre-existing serum rAAVrh74 antibodies at the time of treatment. At 16 or 24 weeks after rAAVrh74.MCK.*GALGT2* treatment, T-cell ELISpot assays for IFN-γ positive spot forming colonies (spf) in PBMCs in response to pooled peptides from either human GALGT2 transgenic protein (Fig. 2E) or rAAVrh74 capsid protein (Fig. 2F) showed some signals above the 50 spf level considered positive. Here again, ELISpot signals were generally lower in prednisone-treated animals. ELISpots from Concanavalin A-treated PBMCs, used as a positive control, always exceeded an average reading of 500 spf/10^6 PBMCs, while DMSO alone, used as a negative control, never exceeded an average reading of 13 spf/10^6 PBMCs. For both serum antibodies (Fig. 2D) and peripheral blood T cells (Fig. 2E and F), the reduced levels found with prednisone at these later treatment time points were not statistically significant due to the small number of samples (two to three macaques per group). This trend, however, suggested an immunosuppressive role for prednisone consistent with the reduced numbers of immune cell infiltrates found in prednisone-treated macaques (Fig. 2C).

Expression of markers for T-cell exhaustion in intramuscular infiltrates

Intramuscular infiltrates primarily consisted of CD8+ cytotoxic T cells (Fig. 3A). Some FOXP3+ Treg cells were also present, as were occasional CD11b+ macrophages and CD4+ T helper cells (Fig. 3A). The presence of CD8+ T-cell infiltrates in rAAVrh74.MCK.*GALGT2*-treated muscles suggested that cytotoxic T-cell responses to transgene or AAV capsid protein were occurring within the treated muscle. *GALGT2* transgene expression, however, remained high in seronegative rAAVrh74.MCK.*GALGT2*-treated muscles, despite the presence of cytotoxic CD8+ T cells (Fig. 1B). Therefore, next, the study explored whether these CD8+ infiltrates were undergoing apoptosis by co-staining with CC3, an antibody that recognizes the activated (cleaved) form of caspase 3, a marker for certain apoptotic cells (Fig. 3B). Indeed, a majority of CD8+ T cells within such infiltrates showed positive staining for activated caspase 3. Activated caspase 3 staining was also present in the remaining infiltrates found in prednisone-treated muscles (Fig. 3B). Next PD1 and its ligands, PDL1 and PDL2, were stained for in both AAV-transduced (Fig. 4A) and non-transduced skeletal muscle (Fig. 4B and C). PD1 is a receptor found on T cells that, upon binding PDL1 or PDL2, can induce T-cell exhaustion and apoptosis.[51,52] Immunostaining for PD1, PDL1, and PDL2 in AAV-treated muscle showed that all three proteins were expressed in CD8+ T cells within infiltrates (Fig. 4A). In non-AAV-treated muscles, PD1 was not expressed, while PDL1 and PDL2 were highly expressed at the NMJ (identified by co-staining with α-bungarotoxin; Fig. 4B). In addition, PDL2 was expressed at low levels along the sarcolemmal membrane of some skeletal myofibers, while PDL1 was expressed in a punctate pattern consistent with its presence on intramuscular fibroblasts, which was confirmed by co-staining with ERTR7 (Fig. 4C). Thus, within skeletal muscle, PD1 expression was specific for immune cells, while PDL1 and PDL2 expression was present in immune cells, NMJs, intramuscular fibroblasts (PDL1), and skeletal myofibers (PDL2). Staining of immune cells in skeletal muscles in group 3 (24-week AAV-treated seronegative; Fig. 4) was similar to staining found in group 5 (24-week AAV-treated seropositive; not shown).

Next, the study determined if AAV treatment of rhesus macaque skeletal muscle would induce increased expression of PD1, PDL1, or PDL2 that might protect transgene-expressing muscle cells from T-cell-mediated immunity. To compare expression of PD1, PDL1, and PDL2 in the AAV-treated and -untreated macaques, time-matched immunostaining images were taken from cohorts treated with rAAVrh74.MCK.*GALGT2* or rAAVrh74.MCK.μDystrophin for 12 weeks or from cohorts treated with rAAVrh74.MCK.*GALGT2* for 24 weeks, with or without prednisone (Fig. 5). μDystrophin (μDys) is a truncated cDNA form of the dystrophin-encoding gene that contains elements needed to protect dystrophin-deficient muscle fibers from injury.[23,53] Animals treated with rAAVrh74.MCK.μDys in addition to animals treated with rAAVrh74.MCK.*GALGT2* were used here to discern if any changes in PD1, PDL1, or PDL2 expression were due to a specific transgene or were rather due to the common presence of the rAAVrh74 capsid protein. As macaques normally express full-length dystrophin in their skeletal muscles, μDys-expressing fibers were identified by staining for a FLAG epitope tag that was expressed on μDys protein. These cohorts were additionally compared to control animals receiving only sham treatment (PBS alone) and contralateral control muscles from rAAVrh74.MCK.*GALGT2*-treated muscles where the transgene was not expressed. The absolute levels of

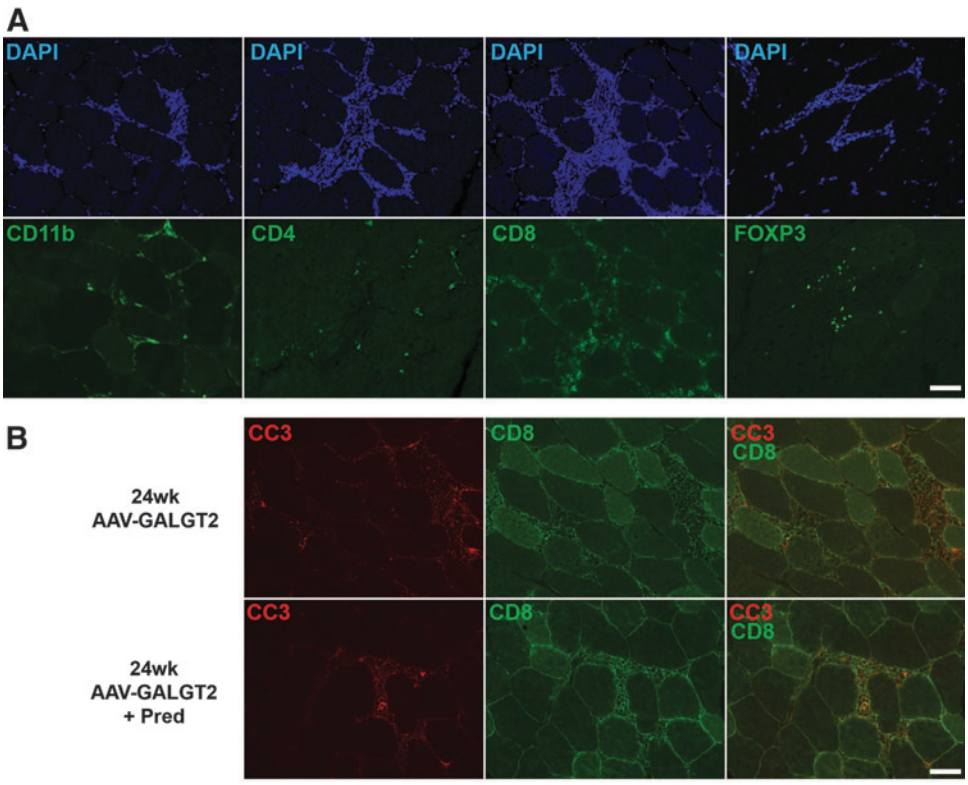

Figure 3. Staining of immune cells in intramusuclar infiltrates. (**A**) Infiltrating mononuclear cells present in rAAVrh74.MCK.*GALGT2*-treated macaque gastrocnemius muscle were stained with monoclonal antibodies to recognize macrophages (CD11b), helper T cells (CD4), cytotoxic T cells (CD8), or regulatory T cells (FOXP3; all *green*). Tissue was costained with DAPI, a marker for cell nuclei, shown in *blue*. Scale bar: 50 μm. (**B**) Infiltrating T cells were co-stained with CD8 (*green*) and CC3 (activated caspase 3, *red*), a marker for apoptosis. Merged image on *right* shows overlap in *yellow/orange*. rAAVrh74.MCK.*GALGT2*-injected muscles treated with or without prednisone (Pred) are compared. Scale bar: 50 μm.

WFA expression in Fig. 5 do not match the averages calculated in Fig. 1B because they are single samples of staining rather than averages of hundreds of stained sections.

PD1 expression was primarily present on immune cell infiltrates and was identified only on such cells in muscles that had been transduced with AAV (Fig. 5A). Muscles that were transduced with AAV expressing either *GALGT2* or μDys showed PD1-positive cells at 12 and 24 weeks post treatment. PD1-positive cells were not present in the image taken from the 24-week rAAVrh74.MCK.*GALGT2*-treated cohort that also received prednisone because such T-cell infiltrates were rarely observed in such muscles. PDL1 was also present in CD8+ T-cell infiltrates (Fig. 5B). When images were taken where such infiltrates were absent, PDL1 staining could also be seen in a punctate intramuscular staining pattern reminiscent of intramuscular fibroblasts (*e.g.*, Fig. 4C). Such punctate PDL1 expression appeared unchanged across all cohorts (Fig. 5B). In contrast to PDL1, PDL2 expression was particularly elevated along the sarcolemmal membranes of skeletal myofibers in regions with high transgene expression (Fig. 5C). PDL2 also showed increased muscle cell expression, albeit less dramatically so, in contralateral muscles where no transgene was present (24-week control and 24-week control + prednisone; Fig. 5C).

The study further assessed the expression of PD1, PDL1, and PDL2 by Western blot (Fig. 6). Identical amounts of muscle protein lysate were separated by SDS-PAGE, transferred to a nitrocellulose membrane, and probed with antibodies to PD1, PDL1, or PDL2. Blots were also probed with an antibody to GAPDH as a control to ensure equal protein loading and transfer. Lymph node whole-cell lysate from a rhesus macaque was also run as a positive control to identify PD1, PDL1, and PDL2 protein. A representative example is shown in Fig. 6A, while quantification of all Westerns for particular 24-week AAV-treated cohorts is shown in Fig. 6B–D for PD1, PDL1, and PDL2, respectively. The immunoblotted proteins identified in skeletal muscle for PD1, PDL1, and PDL2 were

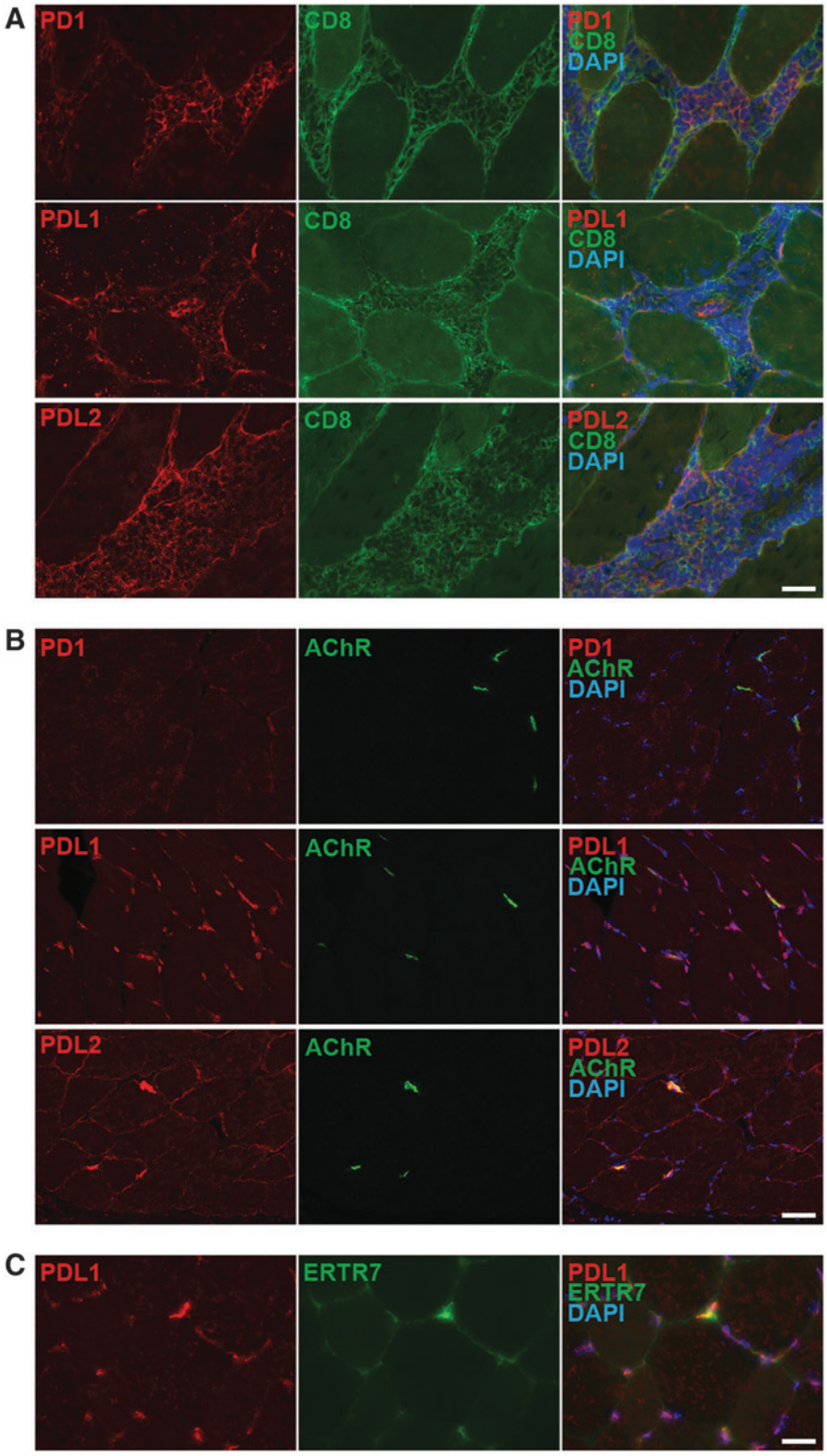

Figure 4. Immunostaining of PD1, PDL1, and PDL2 in AAV-treated and -untreated macaque skeletal muscle. (**A**) Sections of macaque gastrocnemius muscles treated with rAAVrh74.MCK.*GALGT2* containing intramuscular infiltrates were stained to identify overlapping expression of CD8 (*green*) with PD1, PDL1, or PDL2 (all *red*). Merged image is shown at *right*, with DAPI co-staining also shown (*blue*). Scale bar: 25 μm. (**B**) Skeletal muscle that had not been treated with AAV was stained for PD1, PDL1, or PDL2 (*red*) and for α-bungarotoxin (*green*), which stains the neuromuscular junction. Overlap is shown at *right*, with DAPI co-staining in *blue*. Scale bar: 50 μm. (**C**) Skeletal muscle that had not been treated with AAV was stained with PDL1 (*red*) and ERTR7 (*green*), a marker for intramuscular fibroblasts. Merged image is shown at *right*, with DAPI co-staining in *blue*. Scale bar: 25 μm.

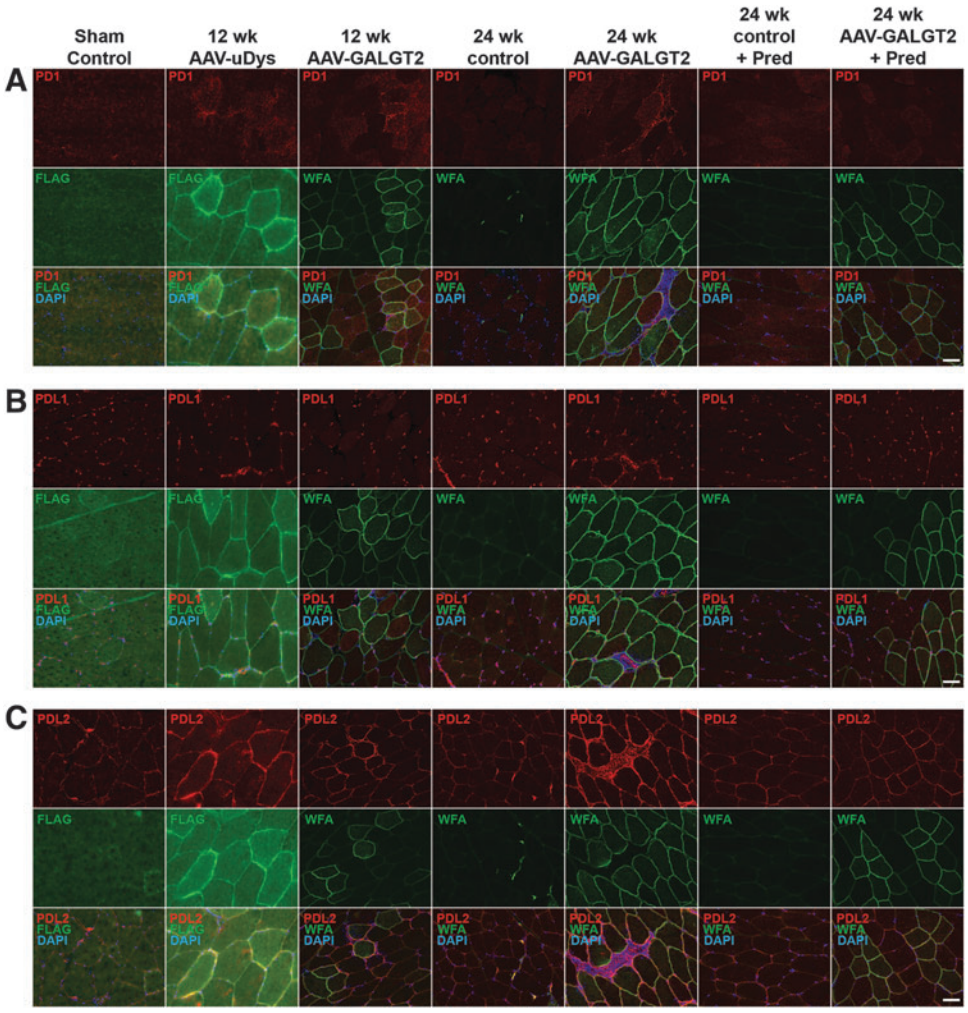

Figure 5. Expression of PD1, PDL1, and PDL2 in AAV-transduced and non-transduced skeletal muscle. Gastrocnemius muscle in the rhesus macaque was treated with phosphate-buffered saline (PBS; sham control), rAAVrh74.MCK.μDystrophin (AAV-μDys), or rAAVrh74.MCK.*GALGT2* (AAV-GALGT2) for 12 or 24 weeks, with or without prednisone (Pred). Contralateral limb muscles from rAAVrh74.MCK.*GALGT2* treated macaques (24-week control and 24-week control + Pred) were also stained. Sections were immunostained for PD1 (**A**), PDL1 (**B**), or PDL2 (**C**), all in *red*, with co-staining for FLAG to identify μDys-expressing myofibers or WFA to identify *GALGT2*-overexpressing myofibers (both *green*). Merged images show overlap in *yellow* below, with DAPI co-staining shown in *blue*. Scale bar: 50 μm.

often present as multiple bands at more than one molecular weight (Fig. 6A). This was also the case for blots of the lymph node cell lysate used as a positive control. While this complicated the interpretation of changes in expression, there was in each instance a primary protein band that represented the majority of the Western blot signal: for example 62 kDa for PD1, 58 kDa for PDL1, and 60 kDa for PDL2. PD1, PDL1, and PDL2 all appear to be heavily glycosylated in a number of cell types and tissues, often doubling their predicted 31–33 kDa molecular weight based on amino-acid sequence and frequently showing multiple protein species.[54–58]

PD1, PDL1, and PDL2 all showed elevated expression at 24 weeks in rAAVrh74.MCK.*GALGT2*-treated muscles relative to all other conditions (Fig. 6A), and this elevation was statistically significant for all three proteins relative to group 1 sham control muscles (Fig. 6B–D). For PD1, muscle protein expression was significantly higher in AAV-treated muscles from macaques that did not receive the prednisone (group 3) compared with those that did receive prednisone (Group 4; Fig. 6B), and PDL1 showed a trend for this difference (Fig. 6C). PDL2 expression was similarly increased by Western blot analysis in the 24-week rAAVrh74.MCK.*GALGT2*-treated group 3 muscle compared with group 1 sham control. PDL2 protein was also overexpressed, though more variably so, in the contralateral muscles from AAV-treated macaques (Fig. 6D). This was the case regardless of prednisone treatment. Thus, unlike PD1 and

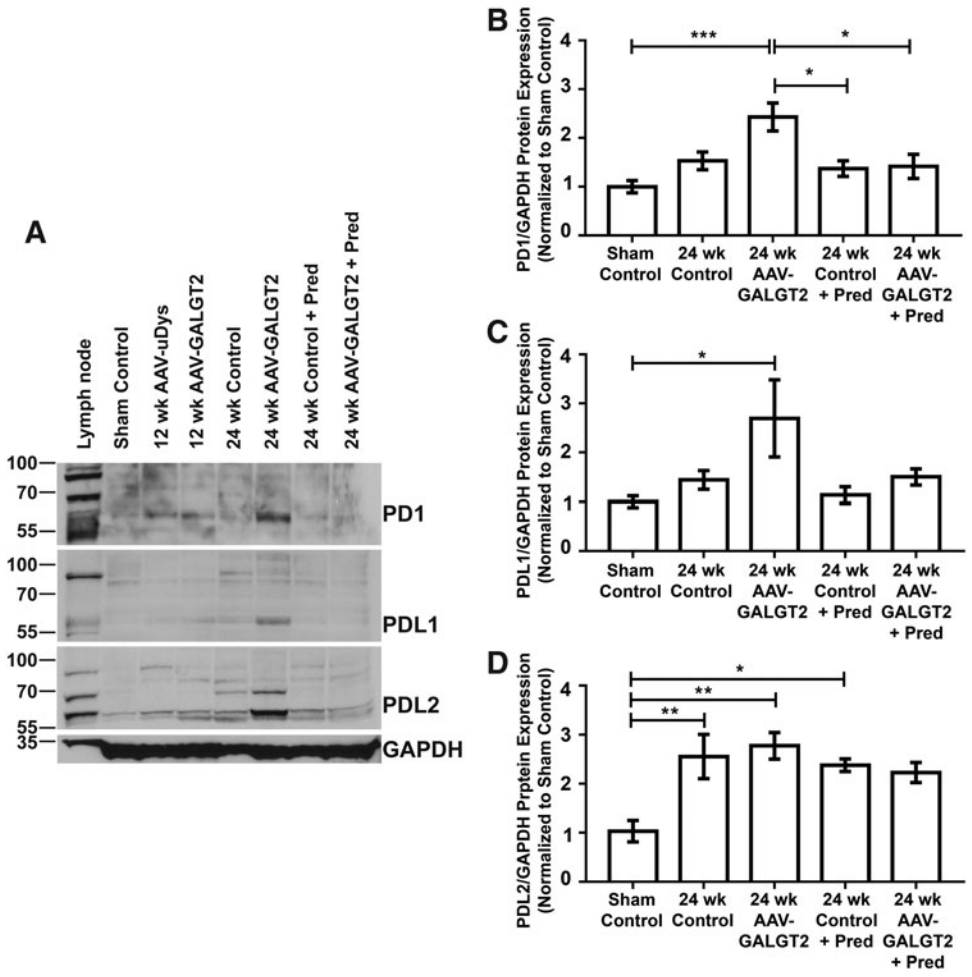

Figure 6. PD1, PDL1, and PDL2 protein expression is upregulated in AAV-transduced skeletal muscle. (**A**) Protein from rhesus macaque lymph node, PBS-treated control skeletal muscle, or AAV-treated gastrocnemius skeletal muscle was separated by SDS-PAGE and immunoblotted for PD1, PDL1, PDL2, or GAPDH. Muscles treated with rAAVrh74.MCK.μDystrophin (AAV-μDys) or rAAVrh74.MCK.*GALGT2* (AAV-GALGT2) for 12 or 24 weeks, with or without prednisone (Pred), were compared to untransduced contralateral muscles from AAV-treated macaques and to PBS-treated (sham control) muscles. Protein expression of PD1 (**B**), PDL1 (**C**), or PDL2 (**D**) was quantified at 24 weeks. Protein amounts were normalized to GAPDH expression in all instances. Data are mean ± SEM for six muscle samples per group, three macaques per group. ***$p < 0.001$; **$p < 0.01$; *$p < 0.05$ using one-way ANOVA.

PDL1, PDL2 protein appeared to be globally induced in muscles where no transgene was present after vascular delivery of AAV.

DISCUSSION

One of the most perplexing aspects of the use of AAV as a gene therapy agent is that high levels of transgene expression can be sustained, even in the presence of T-cell-mediated responses to the gene therapy vector. Many investigators have shown sustained gene expression with a number of genes targeting various tissues in humans and in a number of animal models (*e.g.*, Mingozzi and High,[1] Brantly *et al.*,[5] Mueller *et al.*,[11] Chao *et al.*,[59] Flotte *et al.*,[60] Song *et al.*,[61] Kessler *et al.*,[62] Xiao *et al.*,[63] and Rodino-Klapac *et al.*[64]). In this study, too, sustained expression of the *GALGT2* transgene was observed when delivering rAAVrh74.MCK.*GALGT2* to the gastrocnemius muscle in the rhesus macaque using intravascular AAV delivery.[30] As in a number of other studies, a mounting immune response involving the invasion of CD8+ T cells into treated muscles was observed, even in animals with low pretreatment serum titers to the rAAVrh74 capsid protein.[30] This study shows that these infiltrating CD8+ T cells in AAV-treated muscles express markers of T-cell exhaustion and programmed cell death (PD1 and activated caspase 3). It also shows elevated expression of PD1 ligands, PDL1 and PDL2, in immune infiltrates and elevated expression of PDL2 on skeletal myofibers after systemic AAV delivery. Elevation of PD1 expression in T cells and PDL2 expression in skele-

tal muscle was seen, regardless of the transgene delivered; rAAVrh74 containing the same muscle-specific promoter (MCK) to drive either *GALGT2* or μDystrophin gene expression showed similar findings. Moreover, while PDL2 expression in skeletal myofibers was most increased in regions where transgene overexpression was high, PDL2 protein was also increased, though more variably so, in muscles of AAV-treated macaques where no significant transgene expression was present (*e.g.*, the contralateral limb of a macaque treated only in the other limb using vascular delivery). Elevated PD1 expression on CD8+ T cells and elevated PDL2 expression on skeletal myofibers may be sufficient to drive the majority of intramuscular invading T cells to exhaustion and/or programmed cell death. This, in turn, may provide a privileged environment for sustained transgene expression to AAV-treated skeletal muscle. While PDL1 and PDL2 were also expressed in T cells along with PD1, the presence of PDL2 on skeletal myofibers may allow for trans-PD1 signaling to T cells from the skeletal myofiber. This study corroborates previous studies demonstrating the presence of CD8+ T-cell exhaustion and apoptosis in AAV-transduced skeletal muscle,[65] but additionally describes increased expression of PDL2 along skeletal myofiber membranes after AAV treatment and concentrated expression of both PDL1 and PDL2 at the NMJ in non-AAV-treated macaque muscle. The postsynaptic muscle membrane at the neuromuscular synapse may therefore be less susceptible to T-cell surveillance than the rest of the muscle membrane. Additional cellular mechanisms, for example the presence of infiltrating Treg cells, which can also express PD1 and PDL1, may also impact long-term AAV-mediated gene expression.[6,11,13,66]

The persistence of inert CD8+ T cells observed following treatment with rAAV therapy is reminiscent of what has been seen in hosts undergoing chronic viral infections. Mice that are repeatedly exposed to infectious viruses, such as lymphocytic choriomeningitis virus or polyoma virus, experience failed immunity to the infection due to the exhaustion of CD8+ T cells.[42,67] Similar observations have been made in large animal models, such as chimpanzees infected with hepatitis C or B viruses.[68,69] CD8+ T-cell exhaustion in these instances has been linked to interactions between PD1 and its ligands, PDL1 and PDL2. High levels of PD1 expression on CD8+ T cells are associated with an exhaustion phenotype. In fact, PD1 blockade with anti-PD1 antibodies in a chronic infection model can restore CD8+ T-cell function, resulting in decreased infectivity of the virus.[44,70] With regard to AAV transduction of skeletal muscle, one would want to avoid the reactivation of CD8+ T cells, as T-cell exhaustion can be exploited to maintain therapeutic transgene expression. Alternatively, one could bypass the need for T-cell exhaustion by suppressing the presence of T cells in the AAV-transduced environment, for example with prednisone. This may prove particularly effective in patients with DMD, the disease for which the rAAVrh74.MCK.*GALGT2* gene therapy vector was originally created, as the skeletal muscle exhibits increased inflammation in this disease.

Prednisone immunosuppression is a standard of care therapy for DMD due to the ability of prednisone therapy to prolong ambulation by several years in younger DMD boys.[47] While prednisone does not ultimately impact the long-term progression of DMD disease, it does reduce the incidence of dystrophin self-reactive T cells that can occur in DMD patients.[71] In this study, macaques treated with prednisone prior to AAV delivery had reduced skeletal muscle T-cell infiltration in all instances. This suggests that DMD patients should ideally continue prednisone while receiving gene therapy treatment in order to optimize therapeutic gene expression. Such an immunosuppression regimen could bypass the worry that exhausted CD8+ T cells present in treated skeletal muscles may revert and restore their functional capabilities to attack myofibers expressing the therapeutic transgene. Indeed, the majority of the remaining T-cell infiltrates in prednisone- and AAV-treated muscles still showed high levels of expression for PD1 and activated caspase 3.

Despite reduced AAV vector transduction in macaques treated with prednisone, high glycosylation of muscle by the GALGT2 enzyme was still observed. This may be an added advantage of prednisone, which is a pleiotropic drug. Prednisone, for example, may increase the expression of GALGT2 enzyme substrates such as α dystroglycan. Pereira *et al*. showed that deflazacort, a glucocorticoid similar to prednisone, can increase the expression of dystroglycan protein in dystrophin-deficient muscles.[72] Similar inductive effects of glucocorticoids on skeletal muscle have been shown for utrophin,[73] laminin α2,[74] and integrin α7.[74] While overexpression of *GALGT2* in skeletal muscle alone can increase the expression of many of these same proteins,[24,30,31,75,76] upregulation by prednisone may provide for a combinatorial effect. Indeed, prednisone can alter the expression of hundreds of muscle genes,[77,78] alter protein translation,[79] alter calcineurin/NFAT signaling,[80] and alter Foxo-dependent induction of muscle atrophy genes.[81] Future studies

will be needed to understand these effects, as well as the mechanism by which PDL2 expression in skeletal muscle is increased by AAV. Such studies might uncover additional immunomodulatory mechanisms that could be exploited to optimize particular gene therapies.

ACKNOWLEDGMENTS

This work was supported by NIH grant R01 AR049722 to P.T.M. M.L.C. was supported by a T32 training grant award funded by NIH grant NS077984 and by a graduate training award from the Center for Muscle Health and Neuromuscular Disorders at The Ohio State University. Special thanks to Chris Walker and Bill Bremer (Nationwide Children's Hospital) for performance of T-cell ELISpot assays and to Jerry Mendell for support of the original study.

AUTHOR DISCLOSURE

P.T.M. has a financial conflict of interest with regard to the rAAVrh74.MCK.*GALGT2* vector, as he is the inventor and this technology has been licensed to a corporate interest. The authors have no other conflicts of interest to declare in the submission of this work.

REFERENCES

1. Mingozzi F, High KA. Therapeutic *in vivo* gene transfer for genetic disease using AAV: progress and challenges. Nat Rev Genet 2011;12:341–355.
2. Mingozzi F, High KA. Immune responses to AAV vectors: overcoming barriers to successful gene therapy. Blood 2013;122:23–36.
3. Boisgerault F, Mingozzi F. The skeletal muscle environment and its role in immunity and tolerance to AAV vector-mediated gene transfer. Curr Gene Ther 2015;15:381–394.
4. Nathwani AC, Tuddenham EG, Rangarajan S, et al. Adenovirus-associated virus vector-mediated gene transfer in hemophilia B. N Engl J Med 2011;365: 2357–2365.
5. Brantly ML, Chulay JD, Wang L, et al. Sustained transgene expression despite T lymphocyte responses in a clinical trial of rAAV1-AAT gene therapy. Proc Natl Acad Sci U S A 2009;106: 16363–16368.
6. Nayak S, Sarkar D, Perrin GQ, et al. Prevention and reversal of antibody responses against factor IX in gene therapy for hemophilia B. Front Microbiol 2011;2.
7. Wang L, Cao O, Swalm B, et al. Major role of local immune responses in antibody formation to factor IX in AAV gene transfer. Gene Ther 2005; 12:1453–1464.
8. Arruda VR, Stedman HH, Nichols TC, et al. Regional intravascular delivery of AAV-2-F.IX to skeletal muscle achieves long-term correction of hemophilia B in a large animal model. Blood 2005;105:3458–3464.
9. Herzog RW, Hagstrom JN, Kung SH, et al. Stable gene transfer and expression of human blood coagulation factor IX after intramuscular injection of recombinant adeno-associated virus. Proc Natl Acad Sci U S A 1997;94:5804–5809.
10. Corti M, Elder ME, Falk DJ, et al. B-cell ablation is protective against anti-AAV capsid immune response: a human subject case study. Mol Ther 2014;22:S303–S303.
11. Mueller C, Chulay JD, Trapnell BC, et al. Human Treg responses allow sustained recombinant adeno-associated virus-mediated transgene expression. J Clin Invest 2013;123:5310–5318.
12. Jiang H, Couto LB, Patarroyo-White S, et al. Effects of transient immunosuppression on adenoassociated, virus-mediated, liver-directed gene transfer in rhesus macaques and implications for human gene therapy. Blood 2006;108:3321–3328.
13. Mingozzi F, Hasbrouck NC, Basner-Tschakarjan E, et al. Modulation of tolerance to the transgene product in a nonhuman primate model of AAV-mediated gene transfer to liver. Blood 2007;110: 2334–2341.
14. Spencer HT, Riley BE, Doering CB. State of the art: gene therapy of haemophilia. Haemophilia 2016;22:66–71.
15. Thwaite R, Pages G, Chillon M, et al. AAVrh.10 immunogenicity in mice and humans. Relevance of antibody cross-reactivity in human gene therapy. Gene Ther 2015;22:196–201.
16. Calcedo R, Wilson JM. Humoral immune response to AAV. Front Immunol 2013;4:341.
17. Calcedo R, Vandenberghe LH, Gao G, et al. Worldwide epidemiology of neutralizing antibodies to adeno-associated viruses. J Infect Dis 2009;199:381–390.
18. Murphy SL, Li H, Zhou S, et al. Prolonged susceptibility to antibody-mediated neutralization for adeno-associated vectors targeted to the liver. Mol Ther 2008;16:138–145.
19. Mingozzi F, Chen Y, Edmonson SC, et al. Prevalence and pharmacological modulation of humoral immunity to AAV vectors in gene transfer to synovial tissue. Gene Ther 2013;20:417–424.
20. Sack BK, Merchant S, Markusic DM, et al. Transient B cell depletion or improved transgene expression by codon optimization promote tolerance to factor VIII in gene therapy. PLoS One 2012;7:e37671.
21. Moghimi B, Sack BK, Nayak S, et al. Induction of tolerance to factor VIII by transient coadministration with rapamycin. J Thromb Haemost 2011;9:1524–1533.
22. Nishimura H, Minato N, Nakano T, et al. Immunological studies on PD-1 deficient mice: implication of PD-1 as a negative regulator for B cell responses. Int Immunol 1998;10:1563–1572.
23. Chicoine LG, Montgomery CL, Bremer WG, et al. Plasmapheresis eliminates the negative impact of AAV antibodies on microdystrophin gene expression following vascular delivery. Mol Ther 2014; 22:338–347.
24. Nguyen HH, Jayasinha V, Xia B, et al. Overexpression of the cytotoxic T cell GalNAc transferase in skeletal muscle inhibits muscular dystrophy in mdx mice. Proc Natl Acad Sci U S A 2002; 99:5616–5621.
25. Rodino-Klapac LR, Janssen PM, Montgomery CL, et al. A translational approach for limb vascular delivery of the micro-dystrophin gene without high volume or high pressure for treatment of Duchenne muscular dystrophy. J Transl Med 2007;5:45.
26. Dall'Olio F, Malagolini N, Chiricolo M, et al. The expanding roles of the Sd(a)/Cad carbohydrate antigen and its cognate glycosyltransferase B4GALNT2. Biochim Biophys Acta 2014;1840: 443–453.
27. Dohi T, Yuyama Y, Natori Y, et al. Detection of N-acetylgalactosaminyltransferase mRNA which determines expression of Sda blood group carbohydrate structure in human gastrointestinal mucosa and cancer. Int J Cancer 1996;67:626–631.
28. Martin PT, Scott LJ, Porter BE, et al. Distinct structures and functions of related pre- and postsynaptic carbohydrates at the mammalian neuromuscular junction. Mol Cell Neurosci 1999;13: 105–118.

29. Hoyte K, Kang C, Martin PT. Definition of pre- and postsynaptic forms of the CT carbohydrate antigen at the neuromuscular junction: ubiquitous expression of the CT antigens and the CT GalNAc transferase in mouse tissues. Brain Res Mol Brain Res 2002;109:146–160.

30. Chicoine LG, Rodino-Klapac LR, Shao G, et al. Vascular delivery of rAAVrh74.MCK.GALGT2 to the gastrocnemius muscle of the rhesus macaque stimulates the expression of dystrophin and laminin alpha2 surrogates. Mol Ther 2014; 22:713–724.

31. Xu R, Chandrasekharan K, Yoon JH, et al. Overexpression of the cytotoxic T cell (CT) carbohydrate inhibits muscular dystrophy in the dyW mouse model of congenital muscular dystrophy 1A. Am J Pathol 2007;171:181–199.

32. Xu R, DeVries S, Camboni M, et al. Overexpression of Galgt2 reduces dystrophic pathology in the skeletal muscles of alpha sarcoglycan-deficient mice. Am J Pathol 2009;175:235–247.

33. Tinsley J, Deconinck N, Fisher R, et al. Expression of full-length utrophin prevents muscular dystrophy in mdx mice. Nat Med 1998;4:1441–1444.

34. Moll J, Barzaghi P, Lin S, et al. An agrin minigene rescues dystrophic symptoms in a mouse model for congenital muscular dystrophy. Nature 2001; 413:302–307.

35. Deconinck AE, Rafael JA, Skinner JA, et al. Utrophin-dystrophin-deficient mice as a model for Duchenne muscular dystrophy. Cell 1997;90:717–727.

36. Raith M, Valencia RG, Fischer I, et al. Linking cytoarchitecture to metabolism: sarcolemma-associated plectin affects glucose uptake by destabilizing microtubule networks in mdx myofibers. Skeletal muscle 2013;3:14.

37. Xu R, Singhal N, Serinagaoglu Y, et al. Deletion of Galgt2 (B4GalnT2) reduces muscle growth in response to acute injury and increases muscle inflammation and pathology in dystrophin-deficient mice. Am J Pathol 2015;185:2668–2684.

38. Grady RM, Teng H, Nichol MC, et al. Skeletal and cardiac myopathies in mice lacking utrophin and dystrophin: a model for Duchenne muscular dystrophy. Cell 1997;90:729–738.

39. Xu R, Camboni M, Martin PT. Postnatal overexpression of the CT GalNAc transferase inhibits muscular dystrophy in mdx mice without altering muscle growth or neuromuscular development: evidence for a utrophin-independent mechanism. Neuromuscul Disord 2007;17:209–220.

40. Martin PT, Xu R, Rodino-Klapac LR, et al. Overexpression of Galgt2 in skeletal muscle prevents injury resulting from eccentric contractions in both mdx and wild-type mice. Am J Physiol Cell Physiol 2009;296:C476–488.

41. Thomas PJ, Xu R, Martin PT. B4GALNT2 (GALGT2) Gene therapy reduces skeletal muscle pathology in the FKRP P448L mouse model of limb girdle muscular dystrophy 2I. Am J Pathol 2016;186: 2429–2448.

42. Shin H, Wherry EJ. CD8 T cell dysfunction during chronic viral infection. Curr Opin Immunol 2007; 19:408–415.

43. Riley JL. PD-1 signaling in primary T cells. Immunol Rev 2009;229:114–125.

44. Fuller MJ, Callendret B, Zhu B, et al. Immunotherapy of chronic hepatitis C virus infection with antibodies against programmed cell death-1 (PD-1). Proc Natl Acad Sci U S A 2013;110:15001–15006.

45. Nishimura H, Nose M, Hiai H, et al. Development of lupus-like autoimmune diseases by disruption of the PD-1 gene encoding an ITIM motif-carrying immunoreceptor. Immunity 1999;11: 141–151.

46. Latchman Y, Wood CR, Chernova T, et al. PD-L2 is a second ligand for PD-1 and inhibits T cell activation. Nat Immunol 2001;2:261–268.

47. Mendell JR, Moxley RT, Griggs RC, et al. Randomized, double-blind six-month trial of prednisone in Duchenne's muscular dystrophy. N Engl J Med 1989;320:1592–1597.

48. Xiao X, Li J, Samulski RJ. Production of high-titer recombinant adeno-associated virus vectors in the absence of helper adenovirus. J Virol 1998;72: 2224–2232.

49. Zolotukhin S, Byrne BJ, Mason E, et al. Recombinant adeno-associated virus purification using novel methods improves infectious titer and yield. Gene Ther 1999;6:973–985.

50. Livak KJ, Schmittgen TD. Analysis of relative gene expression data using real-time quantitative PCR and the 2(-Delta Delta C(T)) Method. Methods 2001;25:402–408.

51. Keir ME, Butte MJ, Freeman GJ, et al. PD-1 and its ligands in tolerance and immunity. Annu Rev Immunol 2008;26:677–704.

52. Sharpe AH, Wherry EJ, Ahmed R, et al. The function of programmed cell death 1 and its ligands in regulating autoimmunity and infection. Nat Immunol 2007;8:239–245.

53. Harper SQ, Hauser MA, DelloRusso C, et al. Modular flexibility of dystrophin: implications for gene therapy of Duchenne muscular dystrophy. Nat Med 2002;8:253–261.

54. Agata Y, Kawasaki A, Nishimura H, et al. Expression of the PD-1 antigen on the surface of stimulated mouse T and B lymphocytes. Int Immunol 1996;8:765–772.

55. Ishida M, Iwai Y, Tanaka Y, et al. Differential expression of PD-L1 and PD-L2, ligands for an inhibitory receptor PD-1, in the cells of lymphohematopoietic tissues. Immunol Lett 2002;84:57–62.

56. Pinchuk IV, Saada JI, Beswick EJ, et al. PD-1 ligand expression by human colonic myofibroblasts/fibroblasts regulates CD4+ T-cell activity. Gastroenterology 2008;135:1228–1237, 1237 e1221–1222.

57. Yokosuka T, Takamatsu M, Kobayashi-Imanishi W, et al. Programmed cell death 1 forms negative costimulatory microclusters that directly inhibit T cell receptor signaling by recruiting phosphatase SHP2. J Exp Med 2012;209:1201–1217.

58. Chen BJ, Chapuy B, Ouyang J, et al. PD-L1 expression is characteristic of a subset of aggressive B-cell lymphomas and virus-associated malignancies. Clin Cancer Res 2013;19:3462–3473.

59. Chao H, Samulski R, Bellinger D, et al. Persistent expression of canine factor IX in hemophilia B canines. Gene Ther 1999;6:1695–1704.

60. Flotte TR, Afione SA, Conrad C, et al. Stable *in vivo* expression of the cystic fibrosis transmembrane conductance regulator with an adeno-associated virus vector. Proc Natl Acad Sci U S A 1993;90:10613–10617.

61. Song S, Morgan M, Ellis T, et al. Sustained secretion of human alpha-1-antitrypsin from murine muscle transduced with adeno-associated virus vectors. Proc Natl Acad Sci U S A 1998;95:14384–14388.

62. Kessler PD, Podsakoff GM, Chen X, et al. Gene delivery to skeletal muscle results in sustained expression and systemic delivery of a therapeutic protein. Proc Natl Acad Sci U S A 1996;93:14082–14087.

63. Xiao X, Li J, Samulski RJ. Efficient long-term gene transfer into muscle tissue of immunocompetent mice by adeno-associated virus vector. J Virol 1996;70:8098–8108.

64. Rodino-Klapac LR, Janssen PM, Montgomery CL, et al. A translational approach for limb vascular delivery of the micro-dystrophin gene without high volume or high pressure for treatment of Duchenne muscular dystrophy. J Transl Med 2007; 5:45.

65. Velazquez VM, Bowen DG, Walker CM. Silencing of T lymphocytes by antigen-driven programmed death in recombinant adeno-associated virus vector-mediated gene therapy. Blood 2009;113: 538–545.

66. Josefowicz SZ, Lu LF, Rudensky AY. Regulatory T cells: mechanisms of differentiation and function. Annu Rev Immunol 2012;30:531–564.

67. Zajac AJ, Blattman JN, Murali-Krishna K, et al. Viral immune evasion due to persistence of activated T cells without effector function. J Exp Med 1998;188:2205–2213.

68. Chisari FV, Isogawa M, Wieland SF. Pathogenesis of hepatitis B virus infection. Pathol Biol (Paris) 2010;58:258–266.

69. Rehermann B. Hepatitis C virus versus innate and adaptive immune responses: a tale of coevolution and coexistence. J Clin Invest 2009;119: 1745–1754.

70. Velu V, Titanji K, Zhu B, et al. Enhancing SIV-specific immunity *in vivo* by PD-1 blockade. Nature 2009;458:206–210.

71. Flanigan KM, Campbell K, Viollet L, et al. Anti-dystrophin T cell responses in Duchenne muscular

dystrophy: prevalence and a glucocorticoid treatment effect. Hum Gene Ther 2013;24:797–806.

72. Pereira JA, Marques MJ, Santo Neto H. Co-administration of deflazacort and doxycycline: a potential pharmacotherapy for Duchenne muscular dystrophy. Clin Exp Pharmacol Physiol 2015; 42:788–794.

73. Miura P, Andrews M, Holcik M, et al. IRES-mediated translation of utrophin A is enhanced by glucocorticoid treatment in skeletal muscle cells. PLoS One 2008;3:e2309.

74. Wuebbles RD, Sarathy A, Kornegay JN, et al. Levels of alpha7 integrin and laminin-alpha2 are increased following prednisone treatment in the mdx mouse and GRMD dog models of Duchenne muscular dystrophy. Dis Model Mech 2013;6: 1175–1184.

75. Yoon JH, Johnson E, Xu R, et al. Comparative proteomic profiling of dystroglycan-associated proteins in wild type, mdx, and Galgt2 transgenic mouse skeletal muscle. J Proteome Res 2012;11: 4413–4424.

76. Yoon JH, Chandrasekharan K, Xu R, et al. The synaptic CT carbohydrate modulates binding and expression of extracellular matrix proteins in skeletal muscle: partial dependence on utrophin. Mol Cell Neurosci 2009;41:448–463.

77. Almon RR, DuBois DC, Yao Z, et al. Microarray analysis of the temporal response of skeletal muscle to methylprednisolone: comparative analysis of two dosing regimens. Physiol Genom 2007;30:282–299.

78. Fisher I, Abraham D, Bouri K, et al. Prednisolone-induced changes in dystrophic skeletal muscle. FASEB J 2005;19:834–836.

79. Shah OJ, Kimball SR, Jefferson LS. Acute attenuation of translation initiation and protein synthesis by glucocorticoids in skeletal muscle. Am J Physiol Endocrinol Metab 2000;278:E76–82.

80. St-Pierre SJ, Chakkalakal JV, Kolodziejczyk SM, et al. Glucocorticoid treatment alleviates dystrophic myofiber pathology by activation of the calcineurin/NF-AT pathway. Faseb J 2004;18:1937–1939.

81. Waddell DS, Baehr LM, van den Brandt J, et al. The glucocorticoid receptor and FOXO1 synergistically activate the skeletal muscle atrophy-associated MuRF1 gene. Am J Physiol Endocrinol Metab 2008;295:E785–797.

Received for publication July 22, 2016;
accepted after revision March 17, 2017.

Published online: March 23, 2017.